Available online at www.sciencedirect.com
SCIENCE DIRECT®
C. R. Mecanique 333 (2005) 111–116
COMPTES RENDUS MECANIQUE
http://france.elsevier.com/direct/CRAS2B/

On the slow motion of a cluster of bubbles under the combined action of gravity and thermocapillarity

Antoine Sellier

LadHyX, École polytechnique, 91128 Palaiseau cedex, France

Received 11 August 2004; accepted after revision 11 October 2004
Available online 21 November 2004
Presented by Sébastien Candel

Abstract

The slow migration of N spherical bubbles under combined buoyancy and thermocapillarity effects is investigated by appealing solely to $3N+1$ boundary-integral equations. In addition to the theory and the associated implementation strategy, preliminary numerical results are both presented and discussed for a few clusters involving 2, 3, 4 or 5 bubbles with a special attention paid to the case of rigid configurations. ***To cite this article: A. Sellier, C. R. Mecanique 333 (2005).***

Résumé

Sur la migration d'un ensemble de bulles sous l'action conjuguée de la pesanteur et d'effets thermocapillaires. On détermine la migration de N bulles sphériques sous l'action combinée de la pesanteur et d'effets thermocapillaires par la seule résolution de $3N+1$ équations de frontière. Outre la théorie et sa mise en oeuvre numérique on présente les premiers résultats obtenus pour quelques situations à 2, 3, 4 ou 5 bulles avec une attention particulière pour les configurations rigides. ***Pour citer cet article : A. Sellier, C. R. Mecanique 333 (2005).***
© 2004 Académie des sciences. Published by Elsevier SAS. All rights reserved.

Keywords: Fluid mechanics; Buoyancy; Thermocapillarity; Boundary-integral equations

Mots-clés : Mécanique des fluides ; Sédimentation ; Thermocapillarité ; Équations de frontière

1. Introduction

At least for experimental applications [1] it is worth determining the migration of small spherical bubbles under the combined action of gravity and thermocapillarity. Unfortunately, the available studies [2,3] only address the

E-mail address: sellier@ladhyx.polytechnique.fr (A. Sellier).

1631-0721/$ – see front matter
doi:10.1016/j.crme.2004.10.004

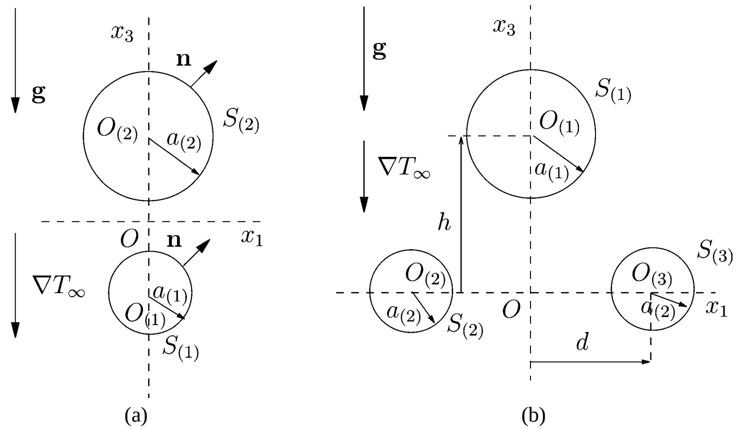

Fig. 1. (a) A 2-bubble and (b) 3-bubble cluster immersed in a Newtonian liquid.

Fig. 1. Cas de (a) deux ou (b) trois bulles plongées dans un liquide Newtonien.

case of two bubbles. This work thus presents a new procedure valid for arbitrary N-bubbles clusters and resorting to $3N+1$ boundary-integral equations. It achieves and tests the numerical implementation of a recent general (arbitrary non-necessarily rigid clusters) theory [4] and pays a special attention to a few rigid falling or ascending clusters of equal or inequal bubbles.

2. Assumptions and governing equations

We consider (see Fig. 1) $N \geqslant 1$ spherical bubble(s) $\mathcal{P}_{(n)}$ with radius $a_{(n)}$, center $O_{(n)}$ and surface $S_{(n)}$ immersed in a Newtonian liquid of uniform viscosity μ and density ρ.

The surface tension $\gamma_{(n)}$ on $S_{(n)}$, high enough to keep $\mathcal{P}_{(n)}$ spherical, depends on the temperature T with $\gamma'_{(n)} = \mathrm{d}\gamma_{(n)}/\mathrm{d}T < 0$ uniform. Cartesian coordinates (O, x_1, x_2, x_3) with $x_i = \mathbf{OM} \cdot \mathbf{e}_i$ are used and the bubbles subject to the uniform gravity field $\mathbf{g} = -g\mathbf{e}_3$ (with $g > 0$) and ambient temperature gradient ∇T_∞ translate without rotating. Therefore, $\mathcal{P}_{(n)}$ experiences an unknown (translational) velocity $\mathbf{U}^{(n)}$ with scale $V_{(n)}$. Assuming [5,6] non-conducting surfaces $S_{(n)}$ and negligible inertial effects ($Re = \rho\,\mathrm{Max}(a_{(n)}V_{(n)})/\mu \ll 1$), the fluid has temperature $T_\infty + T'$, pressure $p + \rho g x_3$ and velocity $\mathbf{u}$ such that

$$\nabla^2 T' = \nabla \cdot \mathbf{u} = 0 \quad \text{and} \quad \mu\nabla^2\mathbf{u} = \nabla p \quad \text{in } \Omega; \quad (\nabla T', \mathbf{u}, p) \to (\mathbf{0}, \mathbf{0}, 0) \quad \text{as } r = |\mathbf{OM}| \to \infty \tag{1}$$

$$\nabla T' \cdot \mathbf{n} = -\nabla T_\infty \cdot \mathbf{n}, \quad \mathbf{u} \cdot \mathbf{n} = \mathbf{U}^{(n)} \cdot \mathbf{n}, \quad \boldsymbol{\sigma} \cdot \mathbf{n} - [\mathbf{n} \cdot \boldsymbol{\sigma} \cdot \mathbf{n}]\mathbf{n} = -\gamma'_{(n)} \nabla_s [T_\infty + T'] \quad \text{on } S_{(n)} \tag{2}$$

with Ω the unbounded liquid domain, $\mathbf{n}$ the unit outward normal on $S_{(n)}$, $\nabla_s[f] = \nabla f - (\nabla f \cdot \mathbf{n})\mathbf{n}$ and $\boldsymbol{\sigma}$ the stress tensor associated to $(\mathbf{u}, p)$. Neglecting inertial effects we determine $(\mathbf{U}^{(1)}, \ldots, \mathbf{U}^{(N)})$ by supplementing (1) and (2) with the relations

$$\mathbf{F}^{(n)} = \int_{S_{(n)}} \boldsymbol{\sigma} \cdot \mathbf{n}\, \mathrm{d}S = 4\pi a_{(n)}^3 \rho \mathbf{g}/3 \quad \text{for } n = 1, \ldots, N \tag{3}$$

For $i = 1, 2, 3$ and $n = 1, \ldots, N$ let us introduce $3N$ Stokes flows $(\mathbf{u}_i^{(n)}, p_i^{(n)})$ with stress tensors $\boldsymbol{\sigma}_i^{(n)}$ obeying the same equations (1) as $(\mathbf{u}, p)$ and the boundary conditions

$$\mathbf{u}_i^{(n)} \cdot \mathbf{n} = \delta_{nm} \mathbf{e}_i \cdot \mathbf{n} \quad \text{and} \quad \boldsymbol{\sigma}_i^{(n)} \cdot \mathbf{n} - [\mathbf{n} \cdot \boldsymbol{\sigma}_i^{(n)} \cdot \mathbf{n}]\mathbf{n} = \mathbf{0} \quad \text{on } S_{(m)} \text{ for } m = 1, \ldots, N \tag{4}$$

with δ the Kronecker symbol. Using the usual tensor summation convention, the unknown quantities $U_j^{(m)} = \mathbf{U}^{(m)} \cdot \mathbf{e}_j$ are then governed [4] by the $3N$-equation linear system

$$\sum_{m=1}^{N} \sum_{j=1}^{3} A_{ij}^{(n),(m)} U_j^{(m)} = \sum_{m=1}^{N} \int_{S_{(m)}} \gamma'_{(m)} (\delta_{nm} \mathbf{e}_i - \mathbf{u}_i^{(n)}) \cdot \nabla_s [T_\infty + T'] \, \mathrm{d}S - \frac{4}{3} \pi a_{(n)}^3 \rho g \delta_{i3} \tag{5}$$

where the occurring coefficients $A_{ij}^{(n),(m)}$ are defined as follows

$$A_{ij}^{(n),(m)} = \int_{S_{(m)}} (\mathbf{e}_j \cdot \mathbf{n})(\mathbf{n} \cdot \boldsymbol{\sigma}_i^{(n)} \cdot \mathbf{n}) \, \mathrm{d}S \tag{6}$$

Since we know ∇T_∞ and $\mathbf{u}_i^{(n)} \cdot \mathbf{n}$ on $S = \bigcup_{m=1}^{N} S_{(m)}$ the unique [4] solution $(\mathbf{U}^{(1)}, \ldots, \mathbf{U}^{(N)})$ to (5) and (6) is readily obtained by solely evaluating on S the vectors $\nabla_s T'$, $\mathbf{a}_i^{(n)} = \mathbf{u}_i^{(n)} - (\mathbf{u}_i^{(n)} \cdot \mathbf{n})\mathbf{n}$ and the function $a_i^{(n)} = \mathbf{n} \cdot \boldsymbol{\sigma}_i^{(n)} \cdot \mathbf{n}/\mu$. Such a key task is detailed in Sections 3 and 4.

3. Relevant boundary-integral equations

The second Green's identity for the harmonic function T' such that $\nabla T' \cdot \mathbf{n} = -\nabla T_\infty \cdot \mathbf{n}$ on S easily yields the well-posed Fredholm boundary-integral equation of the second kind

$$\begin{aligned} -4\pi T'(\mathbf{x}) &+ \int_{S_{(m)}} \left[T'(\mathbf{y}) - T'(\mathbf{x})\right] \frac{(\mathbf{x}-\mathbf{y}).\mathbf{n}(\mathbf{y})}{|\mathbf{x}-\mathbf{y}|^3} \, \mathrm{d}S(\mathbf{y}) + \int_{S \setminus S_{(m)}} T'(\mathbf{y}) \frac{(\mathbf{x}-\mathbf{y}) \cdot \mathbf{n}(\mathbf{y})}{|\mathbf{x}-\mathbf{y}|^3} \, \mathrm{d}S(\mathbf{y}) \\ &= -\int_S \frac{[\nabla T_\infty \cdot \mathbf{n}](\mathbf{y})}{|\mathbf{x}-\mathbf{y}|} \, \mathrm{d}S(\mathbf{y}) \quad \text{for } M \text{ on } S_{(m)} \end{aligned} \tag{7}$$

Note that (7) provides on S not only T' but also the required vector $\nabla_s T'$ by tangential differentiation. When seeking the other desired surface quantities $a_i^{(n)}$ and $\mathbf{a}_i^{(n)}$ it is fruitful to introduce the Oseen–Burgers free-space Green's tensor $\mathbf{G}(\mathbf{y}, \mathbf{x}) = G_{jk}(\mathbf{y}, \mathbf{x}) \mathbf{e}_j \otimes \mathbf{e}_k$ and its associated stress tensor $\mathbf{T}(\mathbf{y}, \mathbf{x}) = T_{kjl}(\mathbf{y}, \mathbf{x}) \mathbf{e}_k \otimes \mathbf{e}_j \otimes \mathbf{e}_l$ such that

$$G_{jk}(\mathbf{y}, \mathbf{x}) = \frac{\delta_{jk}}{|\mathbf{x}-\mathbf{y}|} + \frac{(y_k - x_k)(y_j - x_j)}{|\mathbf{x}-\mathbf{y}|^3}, \qquad T_{kjl}(\mathbf{y}, \mathbf{x}) = -\frac{6(y_k - x_k)(y_j - x_j)(y_l - x_l)}{|\mathbf{x}-\mathbf{y}|^5} \tag{8}$$

Indeed, it can be established starting with the material in [7] that any Stokes flow $(\mathbf{u}', p')$ with stress tensor $\boldsymbol{\sigma}'$ subject to (1) admits on S surface quantities d, $\mathbf{a} = a_k \mathbf{e}_k$, a and $\mathbf{d} = d_k \mathbf{e}_k$ defined as

$$d = \mathbf{u}' \cdot \mathbf{n}, \quad \mathbf{a} = \mathbf{u}' - (\mathbf{u}' \cdot \mathbf{n})\mathbf{n}, \quad a = \mathbf{n} \cdot \boldsymbol{\sigma}' \cdot \mathbf{n}/\mu, \quad \mathbf{d} = \left[\boldsymbol{\sigma}' \cdot \mathbf{n} - (\mathbf{n} \cdot \boldsymbol{\sigma}' \cdot \mathbf{n})\mathbf{n}\right]/\mu \tag{9}$$

that satisfy the following condition and coupled boundary-integral equations

$$\mathbf{a} \cdot \mathbf{n} = \mathbf{0} \quad \text{on } S \quad \text{and} \quad \mathbf{L}_m[a, \mathbf{a}](M) = \mathbf{D}_m[d, \mathbf{d}](M) \quad \text{for } M \text{ on } S_{(m)}, \; m = 1, \ldots, N \tag{10}$$

with, for M on $S_{(m)}$ and $\mathbf{x} = \mathbf{OM} = x_k \mathbf{e}_k$, the following definitions

$$\begin{aligned} \mathbf{L}_m[a, \mathbf{a}](M) = \Bigg\{ & 8\pi a_j(\mathbf{x}) - \int_{S_{(m)}} \left[a_k(\mathbf{y}) - a_k(\mathbf{x})\right] T_{kjl}(\mathbf{y}, \mathbf{x}) n_l(\mathbf{y}) \, \mathrm{d}S(\mathbf{y}) \\ & - \int_{S \setminus S_{(m)}} a_k(\mathbf{y}) T_{kjl}(\mathbf{y}, \mathbf{x}) n_l(\mathbf{y}) \, \mathrm{d}S(\mathbf{y}) + \int_S G_{jk}(\mathbf{y}, \mathbf{x}) n_k(\mathbf{y}) a(\mathbf{y}) \, \mathrm{d}S(\mathbf{y}) \Bigg\} \mathbf{e}_j \end{aligned} \tag{11}$$

$$\mathbf{D}_m[d,\mathbf{d}](M) = \Big\{-8\pi[dn_j](\mathbf{x}) + \int_{S_{(m)}} \{[dn_k](\mathbf{y}) - [dn_k](\mathbf{x})\} T_{kjl}(\mathbf{y},\mathbf{x}) n_l(\mathbf{y})\,\mathrm{d}S(\mathbf{y}) + \int_{S\setminus S_{(m)}} [dn_k](\mathbf{y}) T_{kjl}(\mathbf{y},\mathbf{x}) n_l(\mathbf{y})\,\mathrm{d}S(\mathbf{y}) - \int_S G_{jk}(\mathbf{y},\mathbf{x}) d_k(\mathbf{y})\,\mathrm{d}S(\mathbf{y})\Big\}\mathbf{e}_j \tag{12}$$

Hence, we obtain $a_i^{(n)}$ and $\mathbf{a}_i^{(n)}$ on S by solving (10)–(12) for $d = \delta_{nm}\mathbf{e}_i \cdot \mathbf{n}$ on $S_{(m)}$ and $\mathbf{d} = \mathbf{0}$ on S. In summary, the velocities $\mathbf{U}^{(n)}$ are gained by inverting only the $1 + 3N$ above-mentioned boundary-integral equations (7) and (10)–(12) on the cluster's surface S.

4. Numerical method and results

We define on each $S_{(m)}$ a $N_{(m)}$-node mesh of 6-node isoparametric curvilinear triangular boundary elements [7,8] and a unit vector $\mathbf{c}_{(m)}$ such that the tangential vectors $\mathbf{t}_1 = \mathbf{n} \wedge \mathbf{c}_{(m)}$ and $\mathbf{t}_2 = \mathbf{n} \wedge \mathbf{t}_1$ are non-zero at any nodal point. Thus, S admits $N_t = \sum_{m=1}^{N} N_{(m)}$ nodes at which we set $\mathbf{a}_i^{(n)} = a_i^{(n),1}\mathbf{t}_1 + a_i^{(n),2}\mathbf{t}_2$ (therefore ensuring the condition $\mathbf{a}_i^{(n)} \cdot \mathbf{n} = 0$) with unknown functions $a_i^{(n),1}, a_i^{(n),2}$. Each discretized boundary-integral equation is a linear system, of dense and non-symmetric $N_t' \times N_t'$ influence matrix ($N_t' = N_t$ for (7) and $N_t' = 3N_t$ for ((10)–(12)), which is solved by a LU factorization. The numerical implementation is tested both for a single bubble $\mathcal{P}_{(1)}$ ascending ($\nabla T_\infty = \mathbf{0}$) at the velocity $a_{(1)}^2 \rho g u_s/\mu \mathbf{e}_3$ with [9] $u_s = 1/3$ and two bubbles $\mathcal{P}_{(1)}$ and $\mathcal{P}_{(2)}$ translating for ∇T_∞ parallel to $\mathbf{e}_3$ in absence of gravity at the velocities $\mathbf{U}^{(1)}$ and $\mathbf{U}^{(2)}$. If $\mathbf{O}_{(1)}\mathbf{O}_{(2)}$ is aligned with or normal to $\mathbf{e}_3$ there exist [5,6] four coefficients M_{11}, M_{12}, M_{21} and M_{22} depending on $\lambda = (a_1 + a_2)/O_1O_2$ such that

$$\mathbf{U}^{(1)} = -\frac{[a_{(1)}\gamma_{(1)}' M_{11} + a_{(2)}\gamma_{(2)}' M_{12}]\nabla T_\infty}{2\mu}, \qquad \mathbf{U}^{(2)} = -\frac{[a_{(1)}\gamma_{(1)}' M_{21} + a_{(2)}\gamma_{(2)}' M_{22}]\nabla T_\infty}{2\mu} \tag{13}$$

As shown by Tables 1 and 2 for $a_{(2)} = 2a_{(1)}$ and $\mathbf{O}_{(1)}\mathbf{O}_{(2)} \wedge \mathbf{e}_3 = \mathbf{0}$ (see Fig. 1(a)), the use of 242 collocation points on each bubble yields a quite sufficient precision of order of 0.1% both for distant ($\lambda = 3/23$) or close ($\lambda = 10/11$) bubbles.

Henceforth, $\nabla T_\infty = -\alpha \mathbf{e}_3$ with $\alpha > 0$, $\gamma_{(n)}' = \gamma' < 0$ and $N_{(n)} = 242$. First we consider equal bubbles ($a_{(n)} = a$) located at the vertices of a regular horizontal polygon with $\mathbf{OO}_{(n)} = d(\cos\alpha_{(n)}\mathbf{e}_1 + \sin\alpha_{(n)}\mathbf{e}_2)$, $\alpha_{(n)} = 2\pi(n-1)/N$ and d large enough so that bubbles do not touch. For symmetry reasons $\mathbf{U}^{(n)} = a^2\rho g u/(3\mu)\mathbf{e}_3$ with u the velocity normalized by the settling velocity of a single bubble.

As shown in Fig. 2(a), u is in absence of capillary effects ($\nabla T_\infty = \mathbf{0}$) positive and, due to bubble–bubble interactions, increases with N and a/d. For example, $u \sim 1.8$ for five very close bubbles ($N = 5, d/a = 1.75$). When $\nabla T_\infty = -\alpha \mathbf{e}_3$ is non-zero and strong enough a given cluster ((N, d) prescribed) fall. This occurs if the 'dynamic Bond number' $G_{(n)} = a_{(n)}\rho g/(3\gamma'\alpha)$ [3] is smaller than a critical value G_c plotted in Fig. 2(b) versus d/a for $N = 2, \ldots, 5$. The rigid cluster is at rest for $G_{(1)} = G_c$ and falls or ascends if $G_{(1)} < G_c$ or $G_{(1)} > G_c$,

Table 1
Computed value of u_s for different surface $N_{(1)}$-node meshing of a single settling bubble $\mathcal{P}_{(1)}$

Tableau 1
Estimations numériques de u_s pour différents nombres $N_{(1)}$ de points de collocation sur la surface d'une bulle $\mathcal{P}_{(1)}$ soumise à la seule pesanteur

$N_{(1)}$	74	242	1058	Analytical
u_s	0.33183	0.33301	0.33331	0.33333

Table 2
Effect of mesh refinement for the coefficients M_{11}, M_{12}, M_{21} and M_{22} if $a_{(2)} = 2a_{(1)}$. The results obtained in [5,6] are listed for comparisons

Tableau 2
Influence du choix du maillage sur l'évaluation numérique des coefficients M_{11}, M_{12}, M_{21} et M_{22} pour deux bulles différentes ($a_{(2)} = 2a_{(1)}$). Les résultats obtenus dans [5,6] sont fournis à titre de comparaison

$N_{(n)}$	λ	M_{11}	M_{12}	M_{21}	M_{22}
74	3/23	0.97201	0.00116	0.00015	0.97203
242	3/23	0.99535	0.00074	0.00012	0.99592
1058	3/23	0.99903	0.00067	0.00008	0.99960
[5]	3/23	0.99934	0.00066	0.00008	0.99992
74	10/11	0.59198	0.15698	0.08536	0.95447
242	10/11	0.73274	0.25997	0.04577	0.95183
1058	10/11	0.73099	0.26856	0.04699	0.95266
[6]	10/11	0.73136	0.26864	0.04700	0.95300
[5]	10/11	0.73106	0.26894	0.04650	0.95350

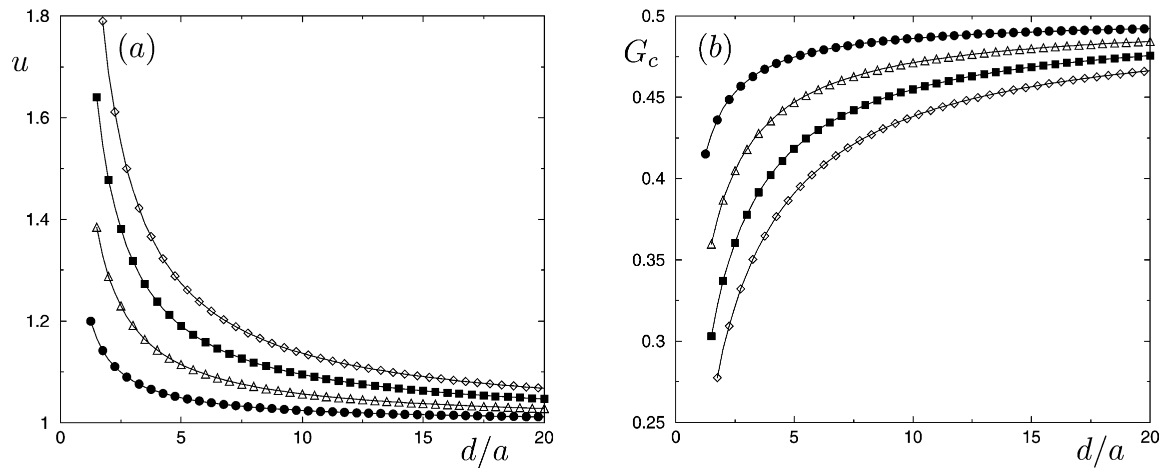

Fig. 2. (a) Normalized velocity u for $\nabla T_\infty = \mathbf{0}$; and (b) critical parameter G_c versus d/a for $N = 2$ (•), $N = 3$ (△), $N = 4$ (■) and $N = 5$ (◊).

Fig. 2. (a) Vitesse adimensionnée u pour $\nabla T_\infty = \mathbf{0}$; et (b) paramètre critique G_c en fonction de d/a pour $N = 24$ (•), $N = 3$ (△), $N = 4$ (■) et $N = 5$ (◊).

respectively. We recover [3] for $N = 2$ and, in full agreement with Fig. 2(a), G_c tends to $1/2$ (case of a single bubble) for d/a large and decreases both with N and a/d.

Let us now consider (see Fig. 1(b)) a big bubble $\mathcal{P}_{(1)}$ located above two smaller bubbles $\mathcal{P}_{(2)}$ and $\mathcal{P}_{(3)}$ with $a_{(2)} = a_{(3)} = a_{(1)}/2$, $\mathbf{OO}_{(1)} = h\mathbf{e}_3$ and $\mathbf{OO}_{(3)} = -\mathbf{OO}_{(2)} = d\mathbf{e}_1$. This time $\mathbf{U}^{(n)} = a_{(2)}^2 \rho g u_{(n)}/(3\mu)\mathbf{e}_3$ with $u_{(2)} = u_{(3)}$. As shown in Fig. 3(a) for $h/a_{(2)} = 5$, $u_{(1)}$ and $u_{(2)}$ deeply depend on $G_{(1)} = a_{(1)}\rho g/(3\gamma'\alpha)$ and $d/a_{(2)} : u_{(1)}$ and $u_{(2)}$ are different and positive (negative) if $d/a_{(2)} \leqslant 15$ for $G_{(1)} = 0.6$ ($G_{(1)} = 0.3$) but $u_{(1)} - u_{(2)}$ changes sign and vanishes at $d/a_{(2)} \sim 8.18$ if $G_{(1)} = 0.45$. Other critical settings (h, d) ensuring $u_{(1)} = u_{(2)}$ exist for $G_{(1)} \in [G_i, G_s]$. Requiring equal velocities for distant bubbles ($d \to \infty$) easily yields $G_i = 1/3$ for $a_{(1)}/a_{(2)} = 2$ and a Newton–Raphson procedure for close bubbles ($d/a_{(2)} = 1.1$) gives G_s and the critical triplets $(d/a_{(2)}, d/h, G_c)$ for which $u_{(1)} = u_{(2)} = 0$. As depicted in Fig. 3(b), the obtained rigid configurations ($u_{(1)} = u_{(2)}$) are falling ($u_{(1)} = u_{(2)} < 0$) for $h/a_{(2)} \geqslant 8.20$ and either falling ($u_{(1)} = u_{(2)} < 0$ if $G_{(1)} \in [G_i, G_c[$), at rest ($u_{(1)} = u_{(2)} = 0$ if $G_{(1)} = G_c$) or ascending ($u_{(1)} = u_{(2)} > 0$ if $G_{(1)} \in]G_c, G_s]$) for $h/a_{(2)} \leqslant 8.20$.

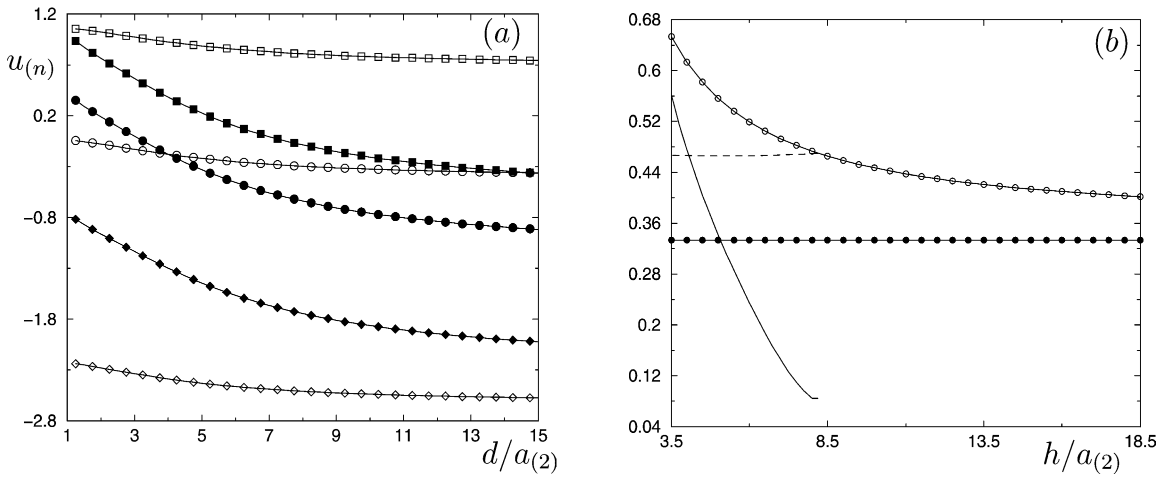

Fig. 3. (a) Normalized velocities $u_{(n)}$ for $h/a_{(2)} = 5$ and $G_{(1)} = 0.30$ ($u_{(1)}$ (◇) and $u_{(2)}$ (♦)), $G_{(1)} = 0.45$ ($u_{(1)}$ (•) and $u_{(2)}$ (○)) and $G_{(1)} = 0.60$ ($u_{(1)}$ (□) and $u_{(2)}$ (■)); (b) Values of G_i (•), G_s (○) and G_c (dashed line). The solid line plots versus $h/a_{(2)}$ the critical ratio $d/(2h)$ for which the cluster is rigid and motionless ($u_{(1)} = u_{(2)} = 0$) when $G_{(1)} = G_c$.

Fig. 3. (a) Vitesses adimensionnées u_n pour $h/a_{(2)} = 5$ et $G_{(1)} = 0,30$ ($u_{(1)}$ (◇) et $u_{(2)}$ (♦)), $G_{(1)} = 0,45$ ($u_{(1)}$ (•) et $u_{(2)}$ (○)) et $G_{(1)} = 0,60$ ($u_{(1)}$ (□) et $u_{(2)}$ (■)) ; (b) Paramètres G_i (•), G_s (○) et G_c (pointillés). La courbe en trait plein trace en fonction de $h/a_{(2)}$ le rapport critique $d/(2h)$ pour lequel le nuage de bulles est indéformable et au repos ($u_{(1)} = u_{(2)} = 0$) lorsque $G_{(1)} = G_c$.

5. Concluding remarks

For arbitrary clusters, the velocity $\mathbf{U}^{(n)}$ of $\mathcal{P}_{(n)}$ is, in general, not necessarily parallel to the gravity direction $\mathbf{g}$ when $\nabla T_\infty \wedge \mathbf{g} = \mathbf{0}$. Such challenging cases, occurring for instance as time evolves for the addressed 3-bubble cluster when $u_{(1)} \neq u_{(2)}$, are currently investigated by exploiting the advocated method. For example, steady 3-bubble configurations translating like a rigid-body at a velocity non-aligned with $\mathbf{g}$ are expected to be found when allowing for this time bubbles of non-equal coefficients $\gamma'_{(n)}$.

References

[1] N.O. Young, J.S. Goldstein, M.J. Block, The motion of bubbles in a vertical temperature gradient, J. Fluid Mech. 197 (1959) 350–356.
[2] R.M. Merritt, D.S. Morton, R.S. Subramanian, Flow structure in bubble migration under the combined action of buoyancy and thermocapillarity, J. Colloid Interf. Sci. 155 (1993) 200–209.
[3] H. Wei, R.S. Subramanian, Migration of a pair of bubbles under the combined action of gravity and thermocapillarity, J. Colloid Interf. Sci. 172 (1995) 395–406.
[4] A. Sellier, On the capillary motion of arbitrary clusters of spherical bubbles. Part 1. General theory, J. Fluid Mech. 197 (2004) 391–401.
[5] M. Meyyappan, W. Wilcox, R.S. Subramanian, The slow axisymmetric motion of two bubbles in a thermal gradient, J. Colloid Interf. Sci. 94 (1983) 243–257.
[6] V.S. Satrape, Interactions and collisions of bubbles in thermocapillary motion, Phys. Fluids A 4 (1992) 1883–1900.
[7] C. Pozrikidis, Boundary Integral and Singularity Methods for Linearized Viscous Flow, Cambridge University Press, 1992.
[8] M. Bonnet, Boundary Integral Equation Methods for Solids and Fluids, Wiley, 1999.
[9] D.D. Joseph, Y.Y. Renardy, Fundamentals of Two-Fluid Dynamics. Part I: Mathematical Theory and Applications, Springer-Verlag, 1991.